

Reports

1979

On basin hyposmetry and the morphodynamic response of coastal inlet systems

John Boon

Robert J. Byrne

Follow this and additional works at: <https://scholarworks.wm.edu/reports>

 Part of the [Oceanography Commons](#)

Archives
GC
97.8
V4
B66
1979

**ON BASIN HYPOMETRY AND THE MORPHODYNAMIC RESPONSE
OF COASTAL INLET SYSTEMS**

by

John D. Boon, III

and

Robert J. Byrne

**Virginia Institute of Marine Science
Gloucester Point, Virginia, U.S.A. 23062**

ABSTRACT

The exchange of water and entrained material between coastal basins and the inner continental shelf reduces to the problem of polarized transport (flood +, ebb -) in the conveyance channels routing flow through a coastal inlet. Here the net long-term movement of materials is largely a function of the fluid velocity and discharge — variables whose time history at-a-station contains both periodic and aperiodic elements. In this paper the importance of the major periodic elements in coastal inlet flows and their potential contribution to the net transport of bedload materials is discussed.

With the aid of a numerical model featuring a closed hypsometric (area-height) representation of basin storage volume, channel flow relationships in a typical basin and inlet system at Wachapreague, Virginia on the East Coast of the United States were studied to determine present mechanisms for inducing net flood or ebb bedload transport. The basin hypsometry and channel dimensions of the prototype system were then varied in the model to simulate other conditions that may have prevailed during earlier stages of basin evolution. Model results show that the principal lunar semidiurnal constituent (M_2) and its first harmonic overtide (M_4) respond in a predictable way to differences in basin hypsometry and channel configuration, and that these constituents in turn account for distinctive rise and fall duration differences observed in the mean tide within the basin. These distortions in basin tides are also reflected at-a-station in the time histories of channel discharge and velocity in the form of greater peak magnitudes during ebb or flood depending upon which phase has the shorter duration, and depending in some instances on a further modulation by basin hypsometry and channel cross-sectional area. A consistent imbalance between peak flows of opposing direction is a plausible mechanism for long-term, net transport of bottom sedimentary materials.

Thus it appears that a systematic contribution toward either flood or ebb dominance in channel flows can arise through complex periodic tides that exist as a result of specific morphological features in basin and inlet systems. The primary significance of these periodic mechanisms may lie in their apparent sensitivity to changes in basin hypsometry.

As the marsh grows, the delta bays are reduced in size resulting in the formation of "finger-like bays" with very sluggish currents. Finally, the partially open lagoon may become entirely marsh filled. Locks recognized that the potential tidal pulse of the system continually diminished throughout the filling sequence and that inlet closure may result.

Based upon studies (Byrnes, et al., 1974) of the Nechanicum Inlet system, Burns and Ford (1976) advanced the speculative hypothesis that some inlet systems may change their bedload transport tendency from flood-dominated, when the lagoon is open, to ebb dominant after lagoon infilling commences. The studies of Bate Oliveira (1970) and Boon (1975) were relevant to the hypothesis. Bate Oliveira observed in the reaches of numerous estuaries that ebb dominant channel transport patterns resulted when basin area varied with tidal stage, a condition to be expected as the lagoon fills. Boon, on the other hand, noted that the relative amplitude and phase of the harmonic "constituents" M_2 , S_2 , F_2 components of the principal lunar tidal constituent (M_2) varied with and tidal duration differences in the vertical tide. In the Nechanicum Inlet case, water level observations with

INTRODUCTION

Studies of the inlet lagoon systems of the New Jersey coast led Lucke (1934) to propose a theory of the evolution of lagoon deposits which form behind a barrier segmented by tidal inlets. The evolutionary sequence is initiated with the formation of flood delta shoals formed by sand advected into the lagoon from the littoral drift system. With continued growth of the shoals, vegetation stabilizes the intertidal portions of shoals and there is contemporaneous incision of the feeder channels between the inlet and lagoon. Ultimately, the primitive flood delta shoals transform into a marsh island complex with distributary channels. As marsh growth proceeds along the fringes of the lagoon, the "delta" marsh complex may couple with the growing delta thus dividing the lagoon into "delta" bays. As the marsh areas enlarge, the delta bays are reduced in size resulting in the formation of "slack-water bays", with very sluggish currents. Finally, the initially open lagoon may become entirely marsh filled. Lucke recognized that the potential tidal prism of the system continually diminished throughout the filling sequence and that inlet closure may result.

Based upon studies (Byrne, et al., 1974) of the Wachapreague Inlet system, Byrne and Boon (1976) advanced the speculative hypothesis that some inlet systems may change their bedload transport tendency from flood dominant, when the lagoon is open, to ebb dominant after lagoon infilling becomes advanced. The studies of Mota Oliveira (1970) and Boon (1975) were germane to the hypothesis. Mota Oliveira observed in the results of numerical modelling that ebb dominated channel transport resulted when basin area varied with tidal stage, a condition to be expected as the lagoon fills. Boon, on the other hand, noted that the relative amplitude and phase of the harmonic "overtides" (M_4 , M_6 , M_8 constituents) of the principal lunar tidal constituent (M_2) caused rise and fall duration differences in the vertical tide. In the Wachapreague Inlet case, where open bays are about 33%

of the total area, the duration differences favored ebb dominant transport. Tidal current measurements confirmed the ebb transport tendency. Additional work with analog and numerical flow models (King, 1974; Seelig and Sorenson, 1978) has demonstrated the importance of varying basin area as a control on inlet hydraulic processes. Other modelers have recently shown the significance of M_2 and M_4 tidal interactions in deriving a differential in peak flows and bottom stress in offshore areas (Pingtree and Griffiths, 1979). Nummedal and Humphries (1978), studying North Inlet, S.C., explain an observed duration differences in ebb and flood currents as a result of varying efficiency in water exchange when the basin area is large (high water) versus lower basin area (low water).

The purpose of this paper is to offer further insight into the tidal hydraulic processes which contribute toward flood or ebb dominance in inlet transport regimes. It is widely recognized that among the factors controlling sediment distribution in tidal inlets, nearshore wave energy and the supply of sand within the littoral drift system outside the inlet may be of primary importance in some localities, whereas tidally-induced transport whose magnitude depends upon the local range in the oceanic tide among other variables, is viewed as a controlling mechanism in other areas. Lucke (1934) was among the first to identify many of these factors and Nummedal and Fischer (1978) recently demonstrated their utility in discriminating inlet types within the German and Georgia Bights. It is apparent, however, that the specific aspects of basin morphology and conveyance channel characteristics, which modify net tidal flow behavior in inlets, have not been fully understood to date and deserve further treatment. In our treatment of this problem, we offer an improved concept over what has been referred to as basin geometry, a term which connotes three spatial dimensions. We suggest instead the term basin hypsometry (the distribution of basin surface area with height) because it involves only two spatial dimensions and because of its direct association with

the continuity equation used in tidal flow computations. We also suggest new innovations for describing temporal flow relationships at fixed locations. For example, many investigators have spoken of a "time-flow asymmetry" in periodic tidal flows which can mean virtually any form of departure from a simple sine wave. Moreover, certain time-velocity relationships have been described in the Lagrangian sense by following the motion of specific water masses (Postma, 1961, p. 176) while others employ the Eulerian representation of the velocity field in describing the time-history of flow at fixed locations (at-a-station). We will show how specific types of periodic flow asymmetries of the latter kind may result and discuss their implications regarding net bedload transport.

(Filtration of flow rates in the sand dunes, ... (Postma, 1978).

Although a formulation of ... of height ... as a result to be a reasonable approximation ... it proved to be unsatisfactory for the description of the ... of the ... of ... a basin of maximum surface ... of ... a given elevational contour, ... height provided the contours remain parallel to ... of ... by drainage, however, ... at lower elevations due to drainage ... the latter instance, the relative ... constant with changing height ... of ... that a linear area-height relationship ... of equal parts of solid rock or ... the bed geometry is shown ... (A, B) affects ... of solid matter ...

BASIN AREA-HEIGHT RELATIONSHIP

Mathematical model investigations of basin and inlet systems have usually treated the basin as a simple storage reservoir for water conveyed by the inlet, assuming that the basin is more or less semicircular in plan and accordingly has a nearly uniform tidal response (constant amplitude and phase of the vertical tide in the basin). Keulegan (1967) modeled systems in which the free surface area of the basin remained constant. Mota Oliveira (1970), King (1974), and Seelig et al. (1977) later introduced models allowing the surface area to vary linearly as a function of tidal height within the basin. The effect of varying the rate of surface area change with height was found to influence the temporal distribution of flow rates in the model inlet to a considerable degree (Seelig and Sorensen, 1978).

Although a formulation of basin surface area as a linear function of height may appear to be a reasonable approximation for modeling purposes, it proves to be unsatisfactory for the description of the geomorphology of closed basins. Given a basin of maximum surface area A (top, Figure 2), the fractional area above a given elevational contour, a/A , will vary linearly with height provided the contours remain parallel as in a basin with plane sides. In natural basins affected by drainage, however, contours are curved and progressively shortened at lower elevations due to drainage convergence (bottom, Figure 2). In the latter instance, the relative rate of change in free surface area cannot remain constant with changing height and will tend to decrease sharply near the point of minimum elevation in the basin. More importantly, figure 2 illustrates that a linear area-height relationship forces the total basin volume to consist of equal parts of solid (rock or sediment) and void (air or water), thus fixing the basin geometry as shown in its plane, dimensionless form. A change in basin dimensions (A , H) effects a scale change but does not alter the relative proportion of solid matter present in the basin defined. Linear constructs are

therefore a poor choice in models which would attempt to portray basins as landforms evolving in response to erosion or filling.

Strahler (1952) described a wide class of erosional landforms using the following formula to describe the hypsometric (area-height) relationship in individual basins:

$$h/H = \left[\frac{A_{\max} - a}{a} \cdot \frac{A_{\min}}{A_{\max} - A_{\min}} \right]^Z$$

where a = basin area lying above elevation contour at height h .

A_{\max} = maximum basin area, A_{\min} = minimum basin area.

h = height above minimum basin elevation.

H = height interval between peak and minimum basin elevation.

Z = positive exponent controlling relative volume of solids in basin (area below hypsometric curve).

The Strahler formula produces a family of sigmoidal curves all of which are defined over the same closed region; each curve has a single point of inflection separating a concave part from a convex part (Figure 5). Boon (1975) modified this formula and applied it to tidal marsh drainage basins, demonstrating that systems differing by an order of magnitude in absolute size could have quite similar hypsometric profiles. The modified formula gives the dimensionless area as

$$a/A = G / \{r + G(1 - r)\} ; G = (1 - h/H)^\gamma \quad (1)$$

where $A = A_{\max}$, $r = A_{\min}/A_{\max}$, and $\gamma = 1/Z$. The parameter r controls the amount of basin curvature in terms of slope at the point of inflection. After determining r and γ empirically (Figure 5), equation (1) can be used to predict water surface area as a function of tidal height as required for numerical modeling of basin and inlet systems. Water surface area corresponding to any height h is found as the difference $a_b = A - a$.

BASIN AND INLET MODEL

As a means of investigating the interaction between basin hypsometry and inlet channel hydraulics, we selected the INLET 2 numerical model developed by Seelig (1976) for use in a large marsh basin complex near Wachapreague, Virginia (Figure 1). Given periodic water level variations in the adjacent ocean, the model predicts inlet velocities, discharge, and basin water levels at fixed increments of time by simultaneously solving the momentum equation for channel flow and the continuity equation, $q(t) = a_b(h)dh/dt$, relating channel discharge to basin area and the rate of change in basin water level. We modified the INLET 2 computer routines to obtain this discharge in accordance with equation (1).

An important feature of INLET 2 is its ability to incorporate more than one basin and connecting channel within the model system. This feature allows for separate treatment of individual marsh basins (sometimes called slack water bays) that commonly drain through a bifurcating network of tidal channels whose terminus is a single barrier inlet reaching the sea. Because of their significant contribution to frictional flow resistance these channels are, in effect, extensions of the main inlet.

We selected Swash Bay (Figure 1) as an example of an individual marsh basin within the Wachapreague complex. As one of several discrete subsystems available, its adaptation to the INLET 2 modeling scheme was simple and straightforward. Area-height information (Figure 3 and Table 1) was obtained by planimetry of the areas lying above a selected number of contours, including a contour which approximates the low-order drainage within marsh areas previously described by Boon (1975). The primary channel conveying most of the storage in Swash Bay was then schematized as shown in figure 4 (sea to bay 1). The length of the prototype channel is approximately 3850 m; the average width and depth are 198 m and 5.4 m, respectively. Figure 4 illustrates the use of spatially-averaged

cell dimensions for velocity and momentum calculations performed in the model. Friction, which determines the head loss between each pair of cell centroid points, is dependent on a preselected value of Manning's n (about 0.025 for this example) which varies as a weak function of the mean cell depth, D_i . Figure 3 also illustrates how two or more segmented channels or "stream tubes" from individual bays can be bundled together to represent channel bifurcation much as it occurs in the prototype system. Flow integrity within stream tubes thus joined is often suggested during an ebbing tide by the presence of longitudinal foam lines, particularly in the vicinity of a major inlet. A net velocity differential between discrete regions of the flow field seen in cross-section may also be reflected in the channel bathymetry (Kjerve, 1978). These observations do not preclude a degree of mixing through dispersive processes initiated by turbulence in the presence of vertical or lateral velocity gradients.

MODEL APPLICATION

The dimensionless area-height data compiled for Swash Bay were plotted as shown in figure 5. A curve fitting these data was selected by trial and error from among the family of curves predicted by equation (1); parameters $r = 0.01$ and $\gamma = 1.8$ gave the desired fit representing present conditions. This curve and three additional curves (Figure 5; $\gamma = 2.5, 3.5, 5.0$) were then used in a series of model runs to simulate hydraulic behavior during an assumed developmental sequence progressing from an open basin with nearly vertical sides ($\gamma = 5.0$) to the present sediment-filled basin ($\gamma = 1.8$). In the absence of data on past configurations of Swash Bay, the curvature parameter $r = 0.01$ was assumed for all runs. All runs were given as input a sinusoidal M_2 tide of 58 cm amplitude as determined from tidal measurements just inside Wachapreague Inlet.

Figure 6 contains the graphic output from the INLET 2 model run given present conditions. This run correctly predicts a slight increase in tidal range

from 116 cm at the channel entrance to 122 cm inside Swash Bay. Although tidal measurements have not been made in Swash Bay, a continuous series of tidal heights recorded over a period of several years is available in nearby Wachapreague, Virginia. The latter station has a mean tidal range of 123 cm. Another result in close agreement with the Wachapreague tide data is the model-predicted difference in duration of rising versus falling tide in Swash Bay. Since Swash Bay is treated solely as a storage reservoir in the model, rise and fall durations are equal to the corresponding durations of flood and ebb flow in the channel. As shown in figure 6, this difference favors a longer flood and shorter ebb during one complete cycle (flood duration is predicted to be approximately 0.8 hour longer than ebb). Given a shorter interval in which to transport the same volume of water, the ebb discharge (dashed curve, Figure 6) attains a significantly greater peak value as compared to the flood. This differential is superposed upon a pronounced time-discharge asymmetry (both discharge maxima are shifted toward high water slack) that already exists as a consequence of rapidly changing basin area near high water (Figure 5, $\gamma = 1.8$).

The mean channel velocity (solid curve, Figure 6) has a time distribution similar to the discharge in the initial run for existing conditions. Mean channel velocity is calculated as the discharge divided by the cross-sectional flow area for each model time step at a section selected by the user. In figure 6 we have selected the channel section nearest Swash Bay; however, due to the relatively small range to depth ratio (about 0.2) in all sections of the present channel, none experiences a very significant change in cross-sectional flow area during the tide cycle. Consequently, peak ebb velocities are predicted to exceed peak flood velocities by about 30% throughout the main Swash Bay channel as it now exists.

Figure 7 illustrates the response of the Swash Bay model given a large reduction in cross-sectional area of the entrance channel relative to the maximum bay

MODEL PREDICTIONS

In attempting to take the Swash Bay system back in time to an earlier stage in its development, we faced the problem of specifying a reasonable set of dimensions for the conveyance channel, assuming there was only one. It is well-known (Keulegan, 1967; King, 1974) that a reduction in channel cross-sectional area creates higher flow impedance which in turn leads to a reduction in the tidal range (tidal prism) admitted to the interior basin. O'Brien (1969) and Jarrett (1976) demonstrated a positive, logarithmic correlation between inlet minimum cross-sectional areas and basin tidal prisms for a number of systems believed to have achieved dynamic equilibrium. The latter work, however, simply demonstrates the degree of association between these variables in equilibrium systems, and does not cast one in the role of predictor and the other in the role of predictand when a change in the system is encountered. Therefore, it seemed reasonable to us to proceed with an ensemble of model runs in which both the basin hypsometry and the channel cross-sectional area would be allowed to vary over a selected range of values without regard to equilibrium conditions. We assumed that the channel length between Swash Bay and Wachapreague Inlet would remain constant with the depth to width relationship following the observations of Mehta (in Winton, 1979). A power law relationship results,

$$D_i = 0.042 B_i^{0.92} \quad (2)$$

defining depth, D_i , and width, B_i , in the i th channel section given the cross-sectional area, $A_i = B_i D_i$ in meters (Figure 4). Since channel cross-sectional area is one of the parameters we allow to vary in our ensemble of model runs, we utilized a dimensionless index, A_c/A_b , where A_c is the mean cross-sectional area of all channel sections and A_b is the maximum basin area as defined in equation (1).

Figure 7 illustrates the response of the Swash Bay model given a large reduction in cross-sectional area of the entrance channel relative to the maximum bay

surface area ($A_c/A_b = 0.78 \times 10^{-5}$), all other parameters remaining as given in figure 6. Figure 7 clearly shows that frictional forces become dominant due to the imposed channel restriction and that the resulting distortion of the basin tide favors a longer ebb rather than flood duration. Adopting the convention of positive flood and negative ebb durations, the duration difference is about -1.0 hour for the run shown in figure 7. As noted previously, the conveyance channel experiences a greater peak discharge during the tidal phase having the shorter duration. However, the time-discharge asymmetry is not pronounced in figure 7 because of the sharp reduction in tidal range within the basin, causing the effect of the basin hypsometry on channel discharge to be lessened. Peak flood velocity in the channel section nearest the basin is about 20% greater than the peak ebb velocity as shown in figure 7; but, due to a much greater range to depth ratio in channel sections nearest the sea, the peak velocity differential in this case reverses itself in seaward sections where discharge and the sea tide are very nearly in phase. In the latter instance velocity is modulated by the temporal change in channel cross-sectional area. Further discussion of this relationship is given later in the paper.

Figure 8 summarizes the results of an ensemble of model runs with respect to tidal duration differences and range reduction within the Swash Bay system. It is readily apparent that basin hypsometry has an important role along with the conveyance channel characteristics in determining the hydraulic behavior of the system. The following relationships are observed:

- (1) A mature or sediment-filled basin ($\gamma = 1.8, 2.5$) having adequate communication with the sea produces positive tidal duration differences. The latter are conducive of greater peak discharge and greater peak velocity during ebb.

- (2) An open basin ($\gamma = 3.5, 5.0$) produces negative tidal duration differences associated with greater peak discharge during flood. Peak channel velocities are dependent upon the degree of tidal range reduction and position within the conveyance channel.
- (3) Major reductions in channel cross-sectional area lead to a reduction in basin tidal range which tends to eliminate the effect of varying basin hypsometry. The tidal duration difference becomes strongly negative for highly restricted channels.
- (4) A filled marsh basin ($\gamma = 1.8$) appears to reach a condition in which positive duration differences are progressively reduced as the channel cross-sectional area nears maximum values. It follows that the right side of the curve for $\gamma = 1.8$ may represent a region favoring dynamic equilibrium; namely, one in which the ebb transport potential or channel flushing capacity seaward varies inversely with channel cross-sectional area. The present Swash Bay system lies within this region.
- (5) As a given basin fills with sediment, its potential tidal prism is continually made smaller. Thus the four basin configurations in figure 8 represent four different magnitudes of water volume seeking to pass through a given channel area indicated on the abscissa. The greater the volume, the greater the effect of channel impedance in reducing the portion that is admitted to the basin. For this reason, filled basins have a delayed reduction in tidal range as the channel cross-sectional area nears minimum values.

As previously stated, the model results are based on varying configurations of the Swash Bay system in which the maximum basin area, conveyance channel length, and oceanic tide range of 58 cm amplitude have been held constant.

TIDAL HARMONIC SIGNATURES

The relationships investigated in our model of an evolving basin and inlet system may be collectively described by the term morphodynamics (Wright, 1976). One of the key expressions of morphodynamic behavior in a system which has reached a particular stage in its evolutionary development is contained in the form of the vertical tide within the basin. This is a fortunate occurrence since tidal records of several months to a year in duration are no longer rare in coastal basins and the characteristics of the so-called "shallow water" tides are now easier to discern quantitatively.

It is a well-known fact that tidal oscillations observed in the sea contain a number of periodic components or constituents that arise from specific astronomical and hydrological causes, along with an aperiodic component stemming from various ephemeral events. Depending upon the relative amplitudes of the major periodic constituents, sea tides are frequently classified as semidiurnal (twice-daily), diurnal (daily), or mixed; these and other constituents taken singly and in combination define many other cycles of longer duration which vary in importance from one area to the next (Defant, 1958; Dronkers, 1964). In characterizing the net long-term behavior of a tidally-induced process, it is convenient to employ a sinusoidal representation of the mean tide or the tide resulting after its integration over a suitable time span taken as a multiple of the dominant constituent period. The mean semidiurnal tide at a given location along the East Coast of the United States can be represented by a harmonic series of the form

$$h(t) = h_o + \sum_{n=1}^{\infty} R_n \cos\left(\frac{2\pi nt}{T} - \theta_n\right) \quad (3)$$

where $h(t)$ = height of tide at time t .

h_0 = height of mean water level above datum.

T = fundamental harmonic period.

R_n = amplitude of n th harmonic.

θ_n = phase of n th harmonic at $t = 0$.

In equation (3), the fundamental harmonic period is taken as 12.42 mean solar hours, the period of the principle lunar semidiurnal constituent designated M_2 . The first harmonic term represents the lunar quarterdiurnal constituent, M_4 , a shallow water tide having a period of 6.21 mean solar hours. Combinations of the fundamental lunar tide and its first harmonic are sufficient to explain most of the rise and fall duration difference normally present in shallow water systems (Schureman, 1958, p. 101; Zetler and Cummings, 1967) Figures 9 and 10 demonstrate graphically the functional dependence of these differences upon both the ratio of the M_2 , M_4 constituent amplitudes and the phase, θ , of the M_4 wave relative to M_2 . This information is usually extracted along with other tidal constants for a fixed location through harmonic analysis of recorded tidal heights.

It should be noted in figures 9 and 10 that the frequency or angular speed of the M_4 constituent is exactly twice that of the M_2 constituent, resulting in a combined wave form that is completely stationary. This is not the case for combinations of most other tidal constituents whose speeds are not related by whole numbers. The addition of the M_2 and M_4 tidal constituents then produces a fixed distortion or signature in the mean semidiurnal tide at the location in question. This distortion varies between two end members due to change in θ :

1) a symmetric distortion (figure 9) and 2) an antisymmetric distortion (figure 10) with respect to symmetry about curve maxima and minima. The former is associated with equal rise and fall durations and unequal maxima and minima. The latter is associated with unequal rise and fall durations and equal maxima

and minima. An antisymmetric distortion favoring longer rise durations is termed positive as is a symmetric distortion producing larger maxima. Both are termed negative in the opposing case (longer fall durations, larger minima).

CHANNEL VELOCITY-TIDAL HARMONIC RELATIONSHIPS

The discharge associated with a simple storage basin is expressed by the continuity equation, $q(t) = a_b(h) dh/dt$. In any section of the channel transmitting this flow, the spatial mean of the velocity may be defined as $[v] = q/a_c$ or

$$[v] = \left(\frac{a_b}{a_c}\right) \frac{dh}{dt} \quad (4)$$

where a_c is the area of the channel cross-section in which $[v]$ is determined.

Defining the basin tide relative to mean water level as

$$h = M_2 \cos\omega t + M_4 \cos(2\omega t - \theta) \quad (5)$$

where $\omega = 2\pi/T$ and M_2, M_4 are the amplitudes of the semidiurnal and quarterdiurnal tide, we obtain after differentiating (5) and substituting in (4)

$$[v] = -\frac{\omega a_b}{a_c} \{ M_2 \sin\omega t + 2M_4 \sin(2\omega t - \theta) \}. \quad (6)$$

Ignoring the quantity $\omega a_b/a_c$ for the moment and noting that the harmonic expressions on the right side of equations (5) and (6) are mutually orthogonal functions, it is clear that if symmetric distortion is present in the vertical tide of the basin, then antisymmetric distortion must be present in the horizontal tide or velocity of the inlet channel and vice versa. Figure 11 shows the relationship when the basin tide is positive symmetric ($\theta = 0$), yielding the corresponding channel velocity as positive antisymmetric. The velocity shown in figure 11, or any function of this velocity, has an identical time-history (flood +, ebb -) proceeding in either direction from a zero crossing. Thus, if the bedload trans-

port potential were given, say, as the cube of the velocity exceeding a certain threshold limit, net transport over a complete tidal cycle would still be zero given a fully antisymmetric horizontal tide of either the positive ($\theta = 0$) or negative ($\theta = 180^\circ$) type. The transport function would, however, greatly augment the velocity differences inherent in any degree of symmetric distortion present in the horizontal tide, be it negative ($0 < \theta < 180^\circ$) favoring ebb or positive ($180^\circ < \theta < 360^\circ$) favoring flood as shown graphically in figure 12.

The time-velocity distortion discussed above is due to the distortion present in the basin tide alone assuming the quantity $\omega a_b/a_c$ remains constant in equation (6). Both a_b (basin area) and a_c (channel cross-sectional area) will vary to some extent about their mean value through time with the same periodicity as the vertical tide. Equation (6) then becomes a compound harmonic expression which can be expanded trigonometrically, as is commonly done in equilibrium tidal analysis, into the sum of a series of simple cosine terms wherein equation (6) is made equivalent to equation (3). Without performing the expansions, one can assess by inspection the more significant of the additional, separate contributions to the distortion in $[v]$ due to periodic variations in a_b and a_c .

The model results indicate mature basin hypsometry serves mainly to intensify positive antisymmetric tendencies in the velocity curves in all channel sections since a_b reaches its most extreme magnitudes in a narrow region about high water slack. Consequently, only minor flood and ebb duration differences are due to the direct effect of basin hypsometry on the horizontal tide. Variations in a_c are more complex. In channel sections nearest the basin, a_c varies almost linearly with the basin tide depending on channel side slope; here it tends to produce a negative antisymmetry in velocity since a_c appears in the denominator of equation (6). Near the sea, a_c varies with the sea tide which, if the channel is small and its impedance high, will tend to be in phase with the inlet

discharge (Figure 7). In the latter situation, a_c will always be smaller during ebb than during flood, producing a negative symmetric distortion in velocity. Neither distortion due to temporal variation in a_c is likely to be very pronounced unless the range to depth ratio in the channel is greater than about 0.2.

In general, then, symmetric distortions in velocity curves are required to produce either a net flood or a net ebb bedload transport based on the velocity potential in channels connected to a tidal basin. With the exception of the special case of a seaward entrance in a highly restricted channel, the required distortion in velocity is determined mainly by corresponding distortions that arise in the basin tide. The degree and sign (positive or negative) of the distortion in basin tides is easily measured in terms of the difference between rise and fall duration, ΔD . A positive value of ΔD is conducive of net ebb transport and a negative value of ΔD is conducive of net flood transport.

COMPARISON OF OBSERVED M_2 AND M_4 HARMONIC CONSTANTS

Tidal data were obtained from the National Ocean Survey (NOS) for three basin and inlet systems along the U.S. East Coast to illustrate the use of harmonic information in discerning some of the morphodynamic differences predicted in figure 8. All of these systems have discrete tidal basins with insignificant freshwater inflow. A harmonic analysis was performed on each 29-day segment of a collection of hourly tidal heights available at various stations using the method of least squares (Boon and Kiley, 1978). The M_2 and M_4 harmonic constants were then plotted as points in figure 12; we purposely arranged for each point to represent a 29-day series (approximately one lunar month) in order to illustrate the degree of variability inherent in monthly estimates of the M_2 , M_4 constants. We proceed with a discussion of the constants for each location.

Wachapreague, Virginia - A Filled Marsh Basin

The Wachapreague tide station lies inside a large marsh-lagoon complex (Figure 1) and, as noted earlier, is representative of several filled marsh basins including Swash Bay that communicate with the Atlantic Ocean through a network of relatively deep and stable channels. The data used were recorded in 1978. The Wachapreague data points in figure 12 clearly reveal the positive ΔD values expected, although they are somewhat smaller than those suggested by the Swash Bay model in figure 8. Part of the reason for the disparity lies in the use of a pure sine wave to represent the mean sea tide in the INLET 2 model on which figure 8 is based; Wallops Island, an ocean station about 30 km north of Wachapreague Inlet, provides two data points (based on 1970 data) in figure 12 suggesting that the ocean tide may initially contain harmonic distortion with a slightly negative ΔD value. The M_4/M_2 amplitude ratio appears to increase by at least a factor of three as the tide progresses into the basin. Wachapreague Inlet is a deep and relatively stable inlet having large ebb delta deposits but lacking flood delta deposits at the present time (Byrne, et al., 1974).

Isle of Wight, Maryland - A Partially Filled Basin

The Isle of Wight tide station is located just north of Ocean City Inlet in Isle of Wight Bay. Records were obtained for several months in 1975 and 1976. This bay has numerous shoals that are exposed during spring lows but has very little marsh development (γ estimated to be between 2.5 and 3.5). The bay tide station has a mean range of 67 cm as compared to 103 cm for Ocean City Pier just outside the inlet, yielding a range reduction ratio of 0.65 for this system which, from the model information in figure 8, suggests that the tidal duration differences, ΔD , should be near zero or perhaps slightly negative within the basin. Isle of Wight data points in figure 12 show general agreement with this prediction in having a spread of ΔD values on either side of zero. Again, the ocean tide outside the

inlet has ΔD values that are slightly negative and the M_4/M_2 amplitude ratio appears to increase by a factor of two inside the basin. There have been recent accumulations of bay shoal deposits immediately north of the inlet but no significant ebb delta deposition outside the inlet. However, a number of man-made modifications to Ocean City Inlet have occurred in recent years including dredging and the construction of a jetty system (Dean and Perlin, 1977).

Murrells Inlet, South Carolina - A Restricted Marsh Basin

A comprehensive tidal survey by NOS provided several months of continuous record in 1975 at eight locations within an elongate marsh basin inside Murrells Inlet. This system is unlike the Wachapreague complex in that its conveyance channels are quite shallow (less than 3 m at maximum depth) and lead to a shallow, unstable inlet with extensive platform shoals at the seaward entrance. Three tide stations near the extreme ends of the basin were selected for harmonic analysis and the results are shown in figure 12. Compared with the ocean station data outside Murrells Inlet, it is evident that the M_4/M_2 amplitude ratio increases 6 to 8 times inside the basin accompanied by ΔD values of between -1.0 and -1.5 hours. The mean range outside Murrells Inlet is 155 cm, reduced to a minimum of 128 cm inside the basin for a range reduction ratio of 0.82. Examining the likely position of the Murrells Inlet system in figure 8, it is evident that basin filling in excess of that in Swash Bay has probably occurred ($\gamma < 1.8$), perhaps aided by the expected peak flood enhancement in distal ends of the conveyance channels due to the magnitude of the negative duration differences. Hubbard (1977) states that tidal flow within the inlet entrance channel is ebb dominant. The Murrells Inlet system is one deserving further study from the point of view of morphodynamics.

SUMMARY AND CONCLUSIONS

In this paper we introduce a modification of Strahler's hypsometric formula to describe nonlinear distributions of surface area with height in coastal basins. Our observations suggest that this formula, which describes the basin in terms of a closed set of area-height dimensions, provides a more realistic means of describing prototype system configurations than the linear approximation generally used in numerical modeling. In particular, it has allowed simulation of the tidal hydraulic response in a basin and inlet system in which the basin is filling through natural processes of sedimentation aided by marsh development.

Using the INLET 2 numerical model of Seelig (1976), results have been obtained which show that both channel configuration and basin hypsometry are controlling factors in determining the characteristics of the mean vertical tide within the basin and the mean horizontal tide in the conveyance channel. The concept of a mean (time-averaged) tide is used to isolate the dominant complex periodic component of the fluid motion; i.e., the lunar semidiurnal tide, M_2 , and its associated overtides, principally the lunar quarterdiurnal tide, M_4 , which causes the coarsest degree of distortion in the fundamental wave and thus accounts for most of the rise and fall or flood and ebb duration differences observed in the mean tide. It is within these distortions that we find systematic flow imbalances capable of producing net flood or ebb sediment transport due to tidal action. Such an imbalance appears favoring the ebb direction when basin infilling becomes advanced without excessive restriction of the conveyance channel. In systems in which basin infilling is not advanced, there appears to be a tendency for flood dominance to occur particularly in landward reaches of the channel. Near inlet entrances, channel configuration and the range to depth ratio may decide the matter of flood or ebb dominance with flood tendencies being augmented in many cases by transport induced by wind waves.

This paper has identified some of the mechanisms which govern mean tidal motions and mean flow imbalances in basin and inlet systems. We offer these insights while recognizing that bedload transport in tidal streams is locally dependent on many additional factors relating to the mechanics of near bottom flows which are beyond the scope of this paper. Moreover, the residual transport of suspended matter is similarly dependent on additional factors although the asymmetry present in tidal currents has been previously identified in the literature as one of the most important (Groen, 1967).

ACKNOWLEDGEMENTS

This work is a result of research sponsored in part by the Virginia Institute of Marine Science Institutional Sea Grant Program, supported by the Office of Sea Grant, NOAA, under grant number NA-79-AA-D-00055. The U.S. Government is authorized to produce and distribute reprints for governmental purposes notwithstanding any copyright notation that may appear hereon.

We are grateful to the Tides and Water Levels Division, Office of Oceanography, NOAA, National Ocean Survey for supplying most of the tide data used in this project.

... and M. Parlin, 1977. ...
 ... A.S.C.R. ...
 ... 1938. Ebb and Flow ...
 ... J.J., 1964. Tidal ...
 ... 1967. On the ...
 ... B.K., 1977. Variations ...
 ... J.P., 1976. Tidal ...
 ... G.R., 1967. Tidal ...
 ... Jr., 1974. The ...
 ... 1978. Bathymetry ...
 ... J.R., 1934. Tidal ...
 ... I.R., 1974. ...

REFERENCES

- Boon, J.D., 1975. Tidal discharge asymmetry in a salt marsh drainage system. *Limnol. Oceanogr.* 20:71-80.
- Boon, J.D. and K.P. Kiley, 1978. Harmonic analysis and tidal prediction by the method of least squares. Special Rpt. No. 186 in Applied Science and Ocean Engineering, Virginia Inst. Marine Science, Gloucester Point, Va., 49 pp.
- Byrne, R.J., J.T. DeAlteris and P.A. Bullock, 1974. Channel stability in tidal inlets: A Case Study. A.S.C.E. Proceedings 14th Coastal Engr. Conf., Copenhagen, Denmark:1585-1604.
- Byrne, R.J. and J.D. Boon, III, 1976. Speculative hypothesis on the evolution of barrier island-inlet-lagoon systems: II, A Case Study, Wachapreague, Virginia. Abstracts, Geol. Soc. Am., NE/SE Section Annual Meeting, 8:159
- Dean, R.G. and M. Perlin, 1977. Coastal engineering study of Ocean City Inlet Maryland. A.S.C.E. Proceedings Coastal Sediments '77, Charleston, S.C.: 520-542.
- Defant, A., 1958. Ebb and Flow, the Tides of Earth, Air, and Water. Univ. Michigan Press, Ann Arbor, 121 pp.
- Dronkers, J.J., 1964. Tidal Computations in Rivers and Coastal Waters. North Holland Publishing Co., Amsterdam, 518 pp.
- Groen, P., 1967. On the residual transport of suspended matter by an alternate tidal current. *Netherlands Jour. Sea Res.*, Groningen, 3:564-574.
- Hubbard, D.K., 1977. Variations in tidal inlet processes and morphology in the Georgia embayment. Tech. Rept. CRD-14, Coastal Res. Div., Dept. of Geology, Univ. of South Carolina, Columbia, S.C., 79 pp.
- Jarrett, J.T., 1976. Tidal prism-inlet area relationships. GITI Rpt. 3, Coastal Engr. Res. Center, Ft. Belvoir, Va., 32 pp.
- Keulegan, G.H., 1967. Tidal flow in entrances; water-level fluctuations of basins in communication with seas. Committee on Tidal Hydraulics, U.S. Army Corps of Engrs., Tech. Bull. No. 14, 89 pp.
- King, D.B., Jr., 1974. The dynamics of inlets and bays. Tech. Rpt. No. 22, College of Engr., Univ. of Florida, Gainesville, 82 pp.
- Kjerfve, B., 1978. Bathymetry as an indicator of net circulation in well mixed estuaries. *Limnol. Oceanogr.*, 23:816-821.
- Lucke, J.B., 1934. Tidal inlets: A theory of evolution of lagoon deposits on shorelines of emergence. *Jour. Geol.*, 42:561-584.
- Mota Oliveira, I.B., 1970. Natural flushing ability in tidal inlets. A.S.C.E. Proceedings 12th Coastal Engr. Conf., Wash. D.C.:1827-1845.

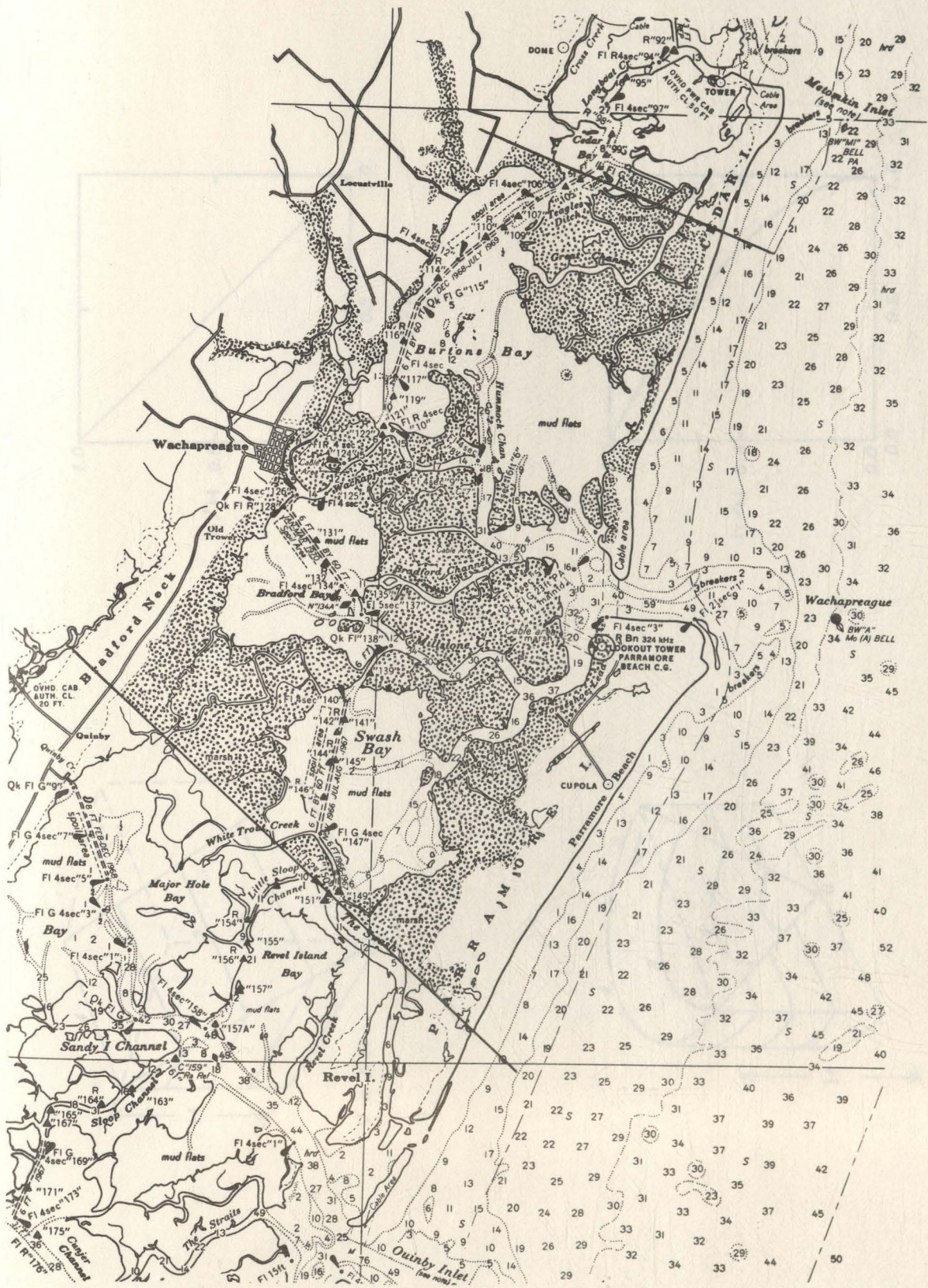
- Nummedal, D. and S.M. Humphries, 1978. Hydraulics and dynamics of North Inlet, South Carolina, 1975-76. GITI Rpt. 16, U.S. Army Coastal Engr. Res. Center, Fort Belvoir, Va., 214 pp.
- Nummedal, D. and I.A. Fischer, 1978. Process-response models for depositional shorelines; the German and the Georgia Bights. A.S.C.E. Proceedings 16th Coastal Engr. Conf., Hamburg, West Germany:1215-1231.
- O'Brien, M.P., 1969. Equilibrium flow areas of inlets on sandy coasts. A.S.C.E. Proceedings, Jour. Waterways and Harbors Div., WWI:43-52.
- Pingtree, R.D. and D.K. Griffiths, 1979. Sand transport paths around the British Isles resulting from M_2 and M_4 tidal interactions. Jour. Mar. Biol. Ass. U.K., 59:497-513.
- Postma, H., 1961. Transport and accumulation of suspended matter in the Dutch Wadden Sea. Netherlands Jour. Sea Res., Groningen, 1:148-190.
- Schureman, P., 1958. Manual of harmonic analysis and prediction of tides. Special Pub. No. 98, U.S. Department of Commerce, Coast and Geodetic Survey, Wash., D.C., 317 pp.
- Seelig, W.N., 1976. Computer program documentation, Inlet 2. Unpublished report, U.S. Army Corps of Engineers, Coastal Engineering Research Center, Fort Belvoir, Va., 37 pp.
- Seelig, W.N., D.L. Harris and B.E. Herchenroder, 1977. A spatially integrated numerical model of inlet hydraulics. GITI Rpt. 14, Coastal Engr. Res. Center, Fort Belvoir, Va., 99 pp.
- Seelig, W.N. and R.M. Sorensen, 1978. Numerical model investigation of selected tidal inlet-bay system characteristics. A.S.C.E. Proceedings 16th Coastal Engr. Conf., Hamburg, West Germany:1302-1319.
- Strahler, A.N., 1952. Hypsometric (area-altitude) analysis of erosional topography. Bull. Geol. Soc. Am., 63:1117-1142.
- Winton, T.C., 1979. Long and short term stability of small tidal inlets. M.S. Thesis, College of Engr., Univ. of Florida, Gainesville, 135 pp.
- Wright, L.D., 1976. Morphodynamics of a wave-dominated river mouth. A.S.C.E. Proceedings 15th Coastal Engr. Conf., Honolulu, Hawaii:1721-1737.
- Zetler, B.D. and R.A. Cummings, 1967. A harmonic method for predicting shallow-water tides. Jour. Mar. Res., 25:103-114.

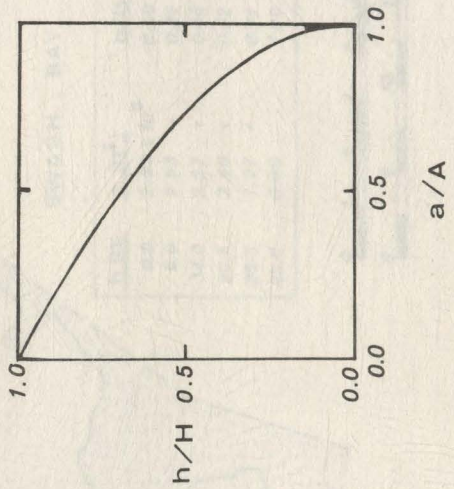
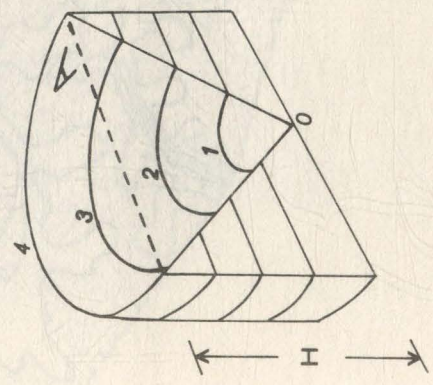
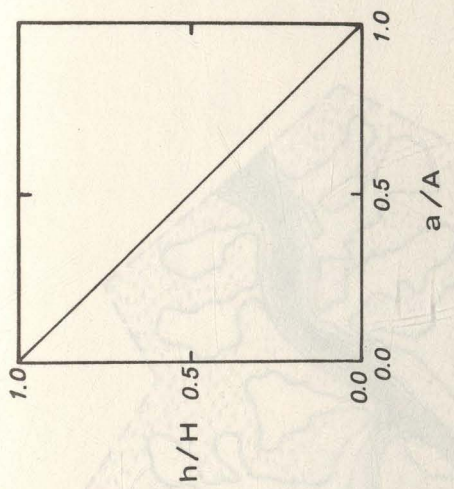
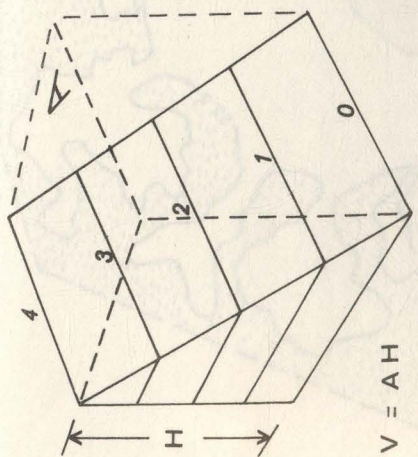
Table 1. Swash Bay Area-Height Data

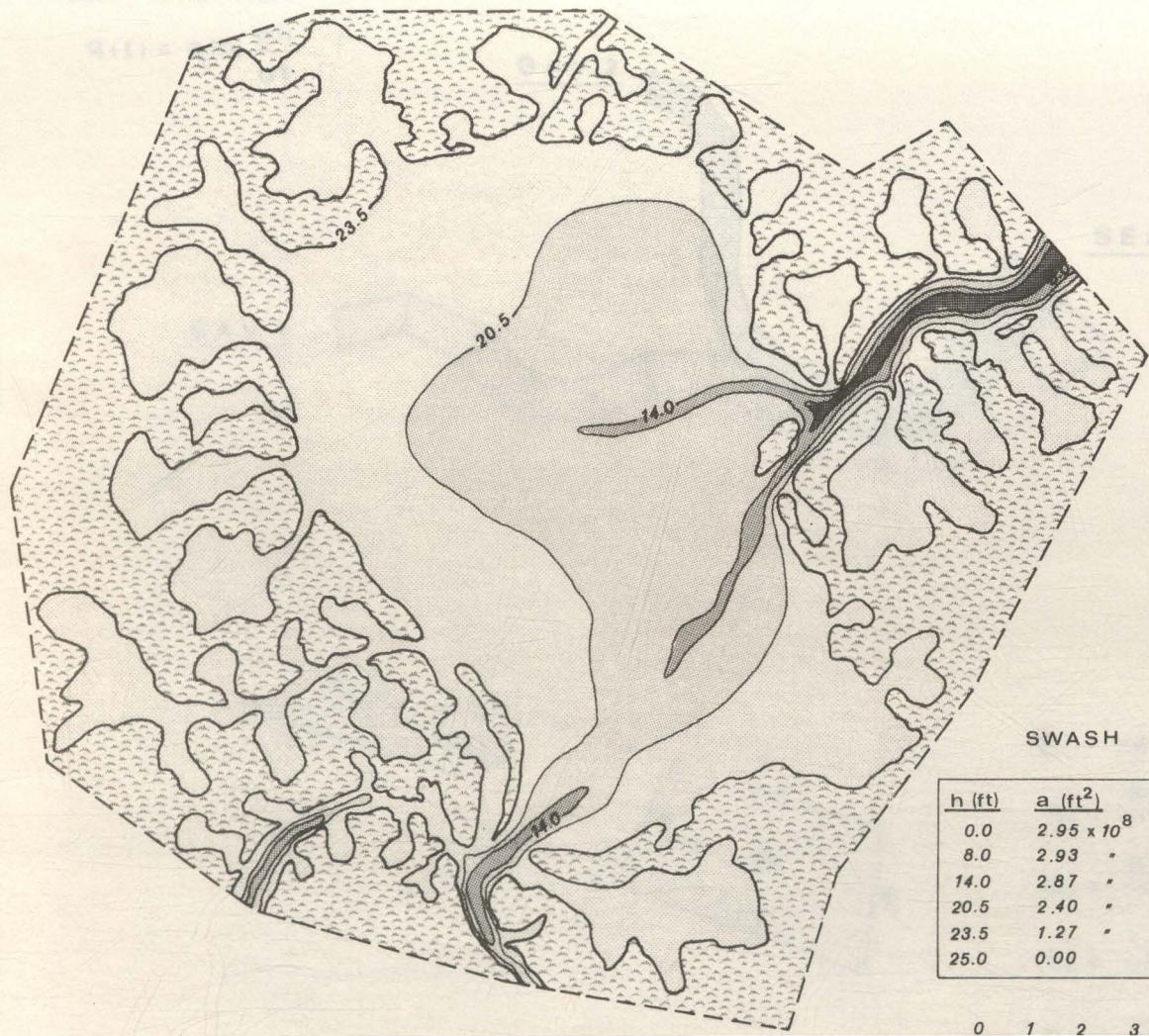
<u>h(m)</u>	<u>a(m² X 10⁶)</u>	<u>h/H</u>	<u>a/A</u>
0.00	27.4	0.00	1.00
2.44	27.2	0.32	0.99
4.27	26.7	0.56	0.97
6.25	22.3	0.82	0.81
7.16	11.8	0.94	0.43
7.62	00.0	1.00	0.00

LIST OF FIGURES

- Figure 1. Map showing the Wachapreague marsh lagoon complex and Swash Bay.
- Figure 2. Schematic examples of the area-height relationship in closed basins. Upper diagrams illustrate a linear relationship, lower diagrams illustrate a nonlinear relationship.
- Figure 3. Areal representation of Swash Bay drainage basin.
- Figure 4. Schematization of Swash Bay channel for use in INLET 2 numerical model.
- Figure 5. Area-height diagram showing four possible basin configurations for Swash Bay; top curve ($\gamma = 1.8$) represents present basin. Shaded area to the right of each curve represents the tidal prism associated with each basin configuration.
- Figure 6. Model results for Swash Bay as presently configured ($\gamma = 1.8$, $A_c/A_b = 3.9 \times 10^{-5}$; $M_2 = 58$ cm, $T = 12.42$ hours); velocity curve shown is for channel section nearest basin.
- Figure 7. Model results for Swash Bay given a restricted entrance channel ($\gamma = 1.8$, $A_c/A_b = 0.78 \times 10^{-5}$; $M_2 = 58$ cm, $T = 12.42$ hours); velocity curve shown is for channel section nearest basin.
- Figure 8. Model results for Swash Bay. Tidal duration differences between flood (+) and ebb (-) phases and range ratios between basin and sea tides are given as a function of the dimensionless cross-sectional area of the conveyance channel for four examples of basin hypsometry.
- Figure 9. Combination of principal lunar semidiurnal constituent, M_2 , with its first harmonic, M_4 . Rise and fall durations are equal given a phase displacement of 0° . Curve distortion is positive symmetric with respect to maxima and minima.
- Figure 10. Combination of principal lunar semidiurnal constituent, M_2 , with its first harmonic, M_4 . Rise duration exceeds fall duration given a phase displacement of 90° . Curve distortion is positive anti-symmetric with respect to maxima and minima.
- Figure 11. Plot of orthogonal harmonic functions (a) $M_2 \cos \omega t + M_4 \cos(2\omega t - \theta)$ and (b) $-M_2 \sin \omega t - 2M_4 \sin(2\omega t - \theta)$ when $\theta = 0^\circ$. Curve (a) is positive symmetric, curve (b) is positive antisymmetric. Given $\theta = 90^\circ$, curve (a) would become positive antisymmetric and curve (b) would become negative symmetric.
- Figure 12. Diagram of tidal duration differences predicted using $M_2 + M_4$ tide model. The duration difference, ΔD , is given as a function of the M_4/M_2 amplitude ratio and phase difference, θ . Each point symbol represents data from a 29-day harmonic analysis at the station indicated.



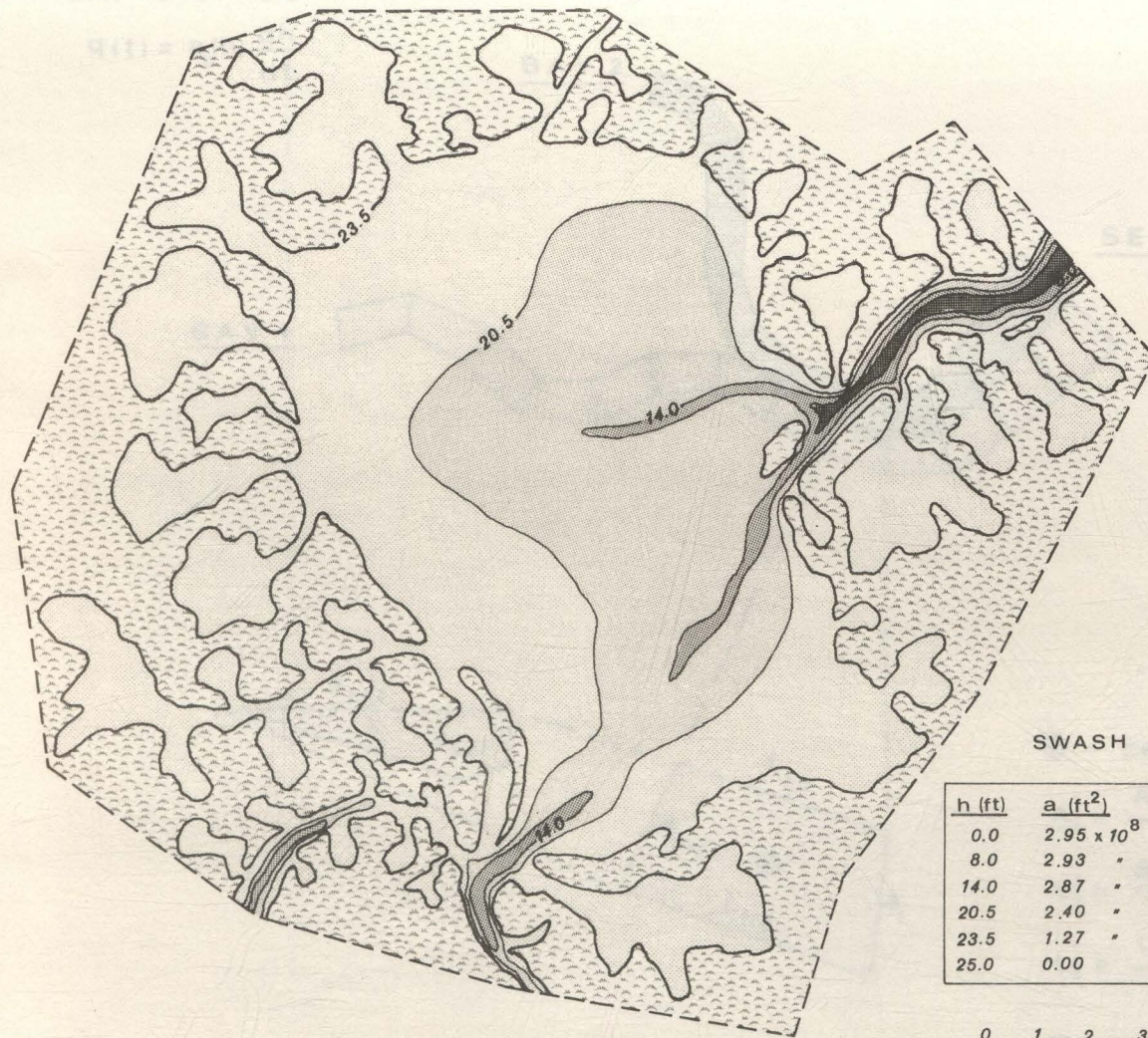




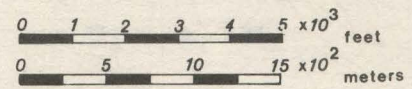
SWASH BAY

h (ft)	a (ft ²)	h/H	a/A
0.0	2.95×10^8	0.00	1.00
8.0	2.93 "	0.32	0.99
14.0	2.87 "	0.56	0.97
20.5	2.40 "	0.82	0.81
23.5	1.27 "	0.94	0.43
25.0	0.00	1.00	0.00

0 1 2 3 4 5 $\times 10^3$

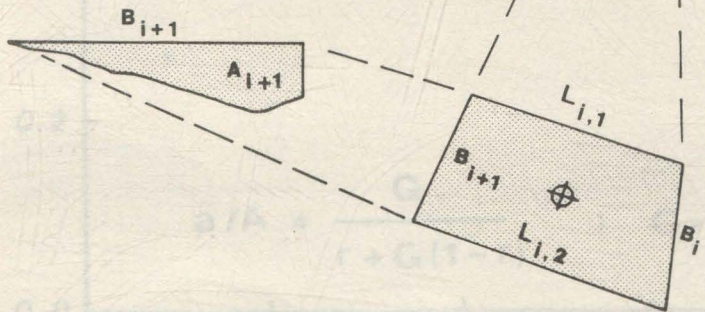
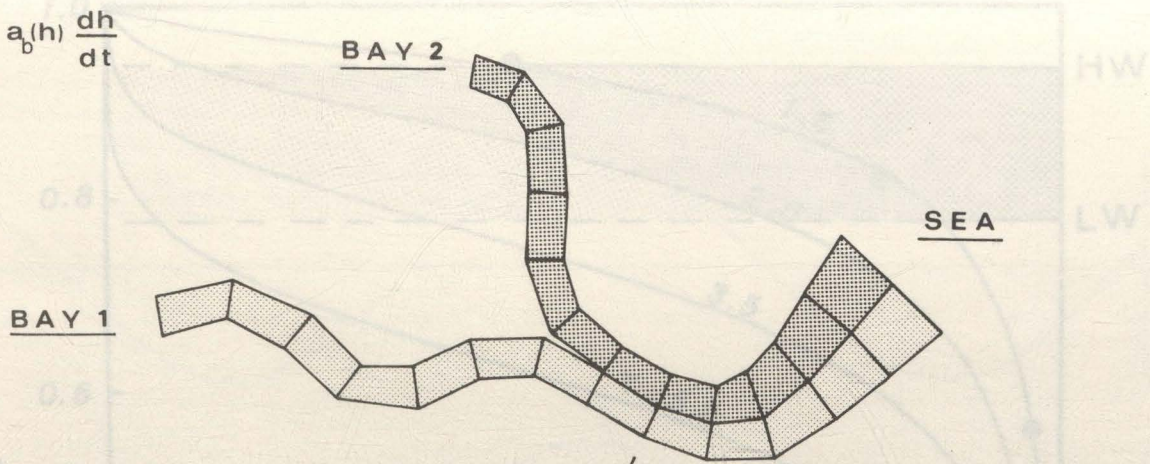


h (ft)	a (ft ²)	h/H	a/A
0.0	2.95×10^8	0.00	1.00
8.0	2.93 "	0.32	0.99
14.0	2.87 "	0.56	0.97
20.5	2.40 "	0.82	0.81
23.5	1.27 "	0.94	0.43
25.0	0.00	1.00	0.00



BAY STORAGE

$$q(t) = a_b(h) \frac{dh}{dt}$$



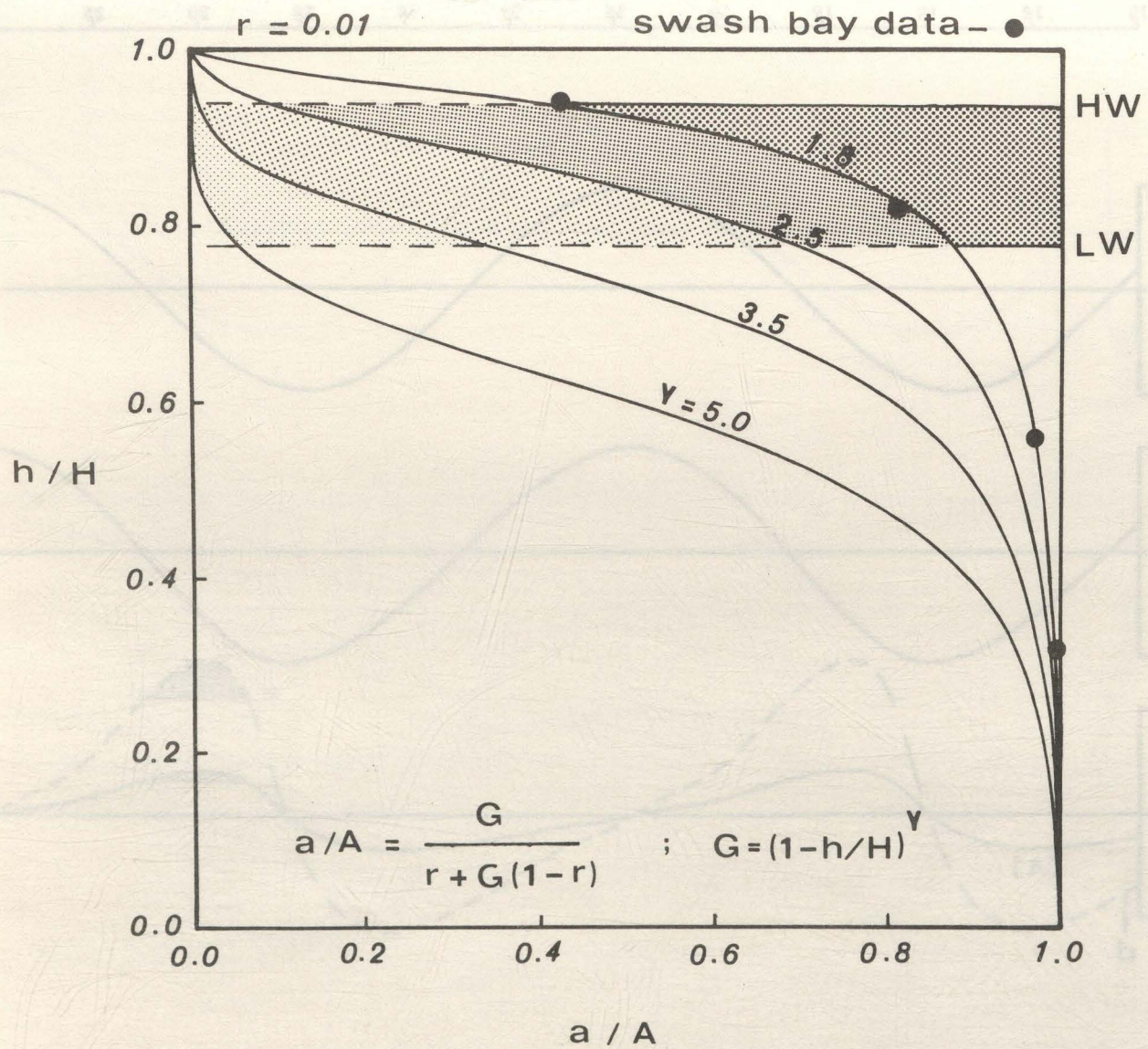
⊕ - cell centroid

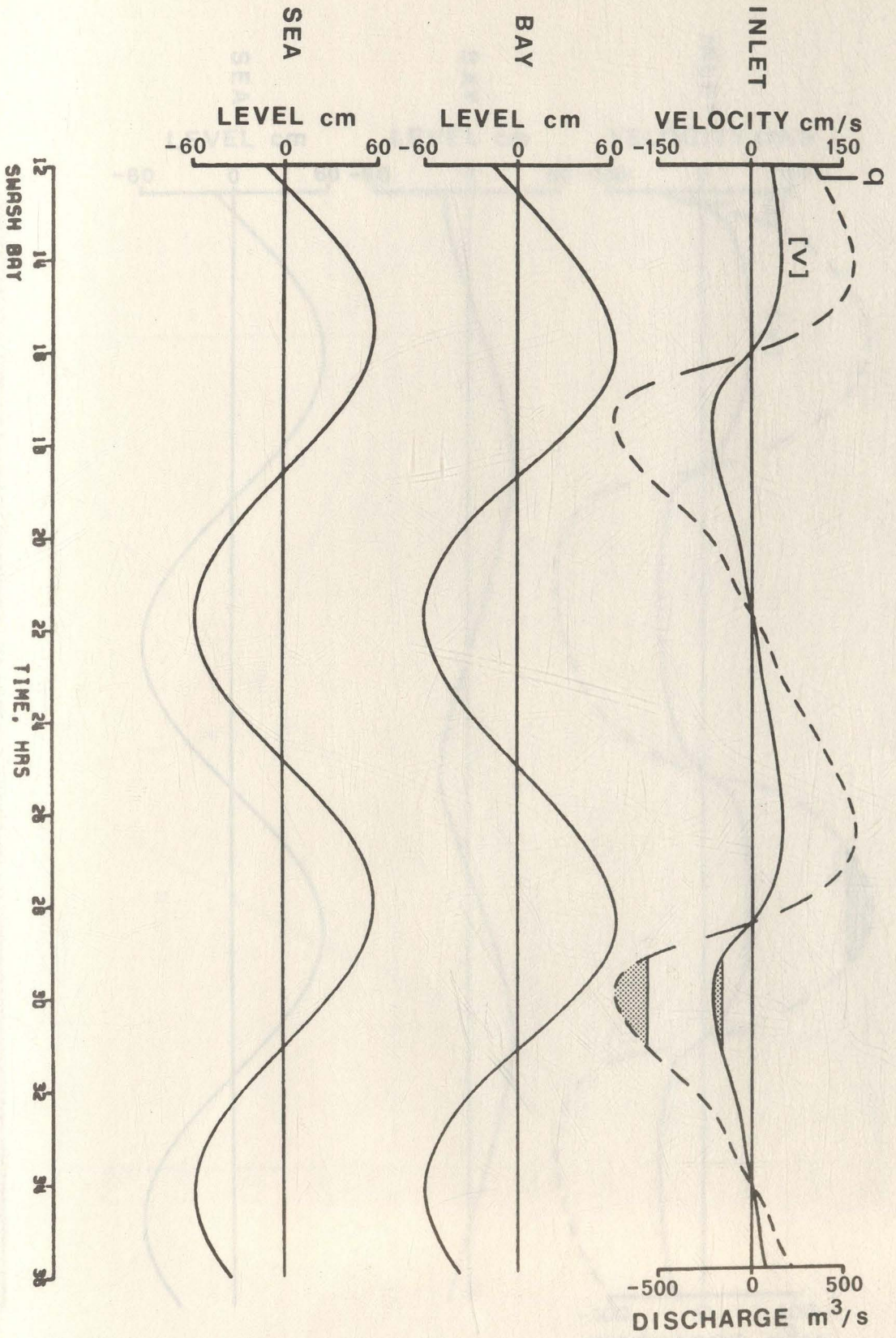
$$A'_i = \frac{A_i + A_{i+1}}{2}$$

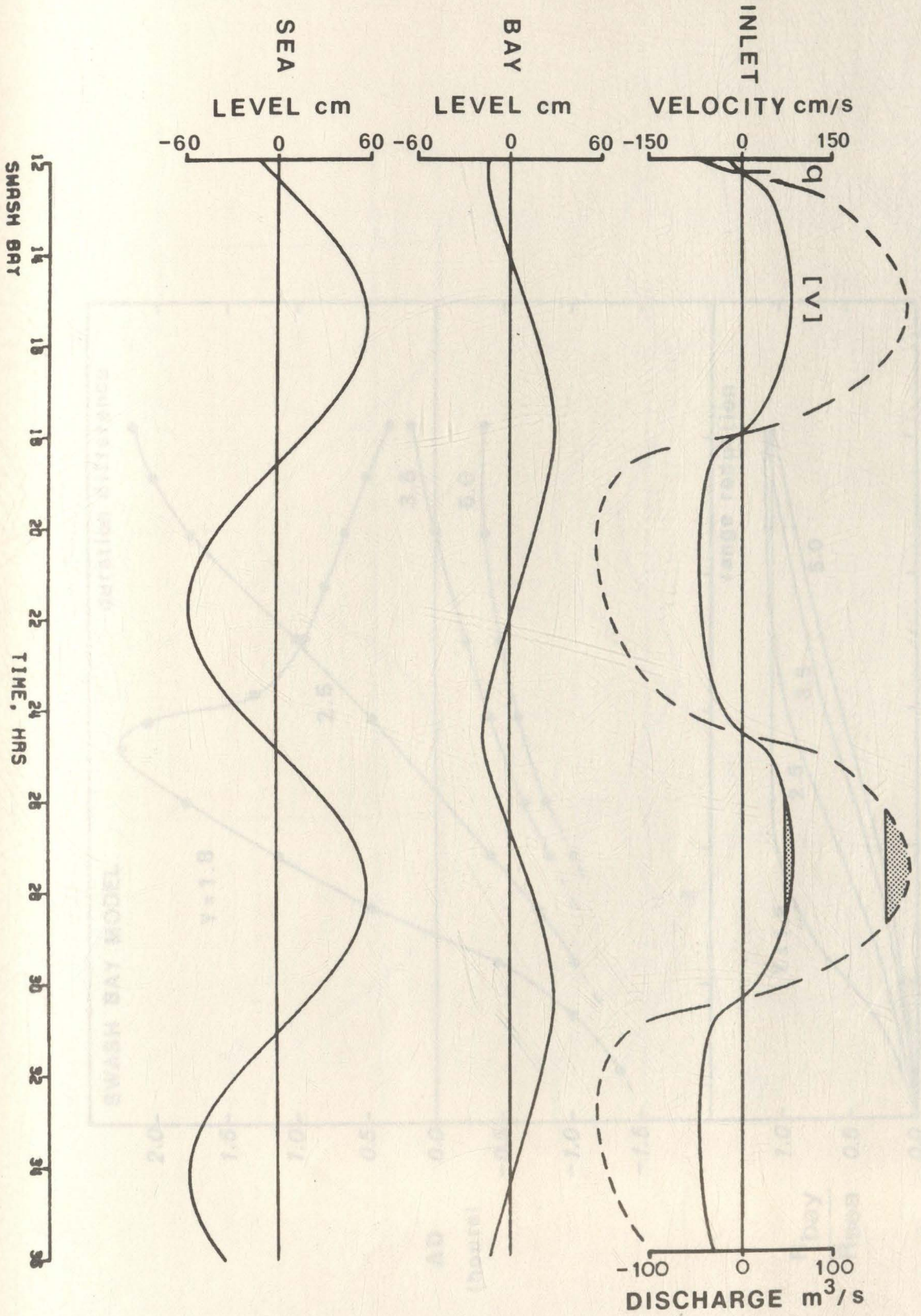
$$B'_i = \frac{B_i + B_{i+1}}{2}$$

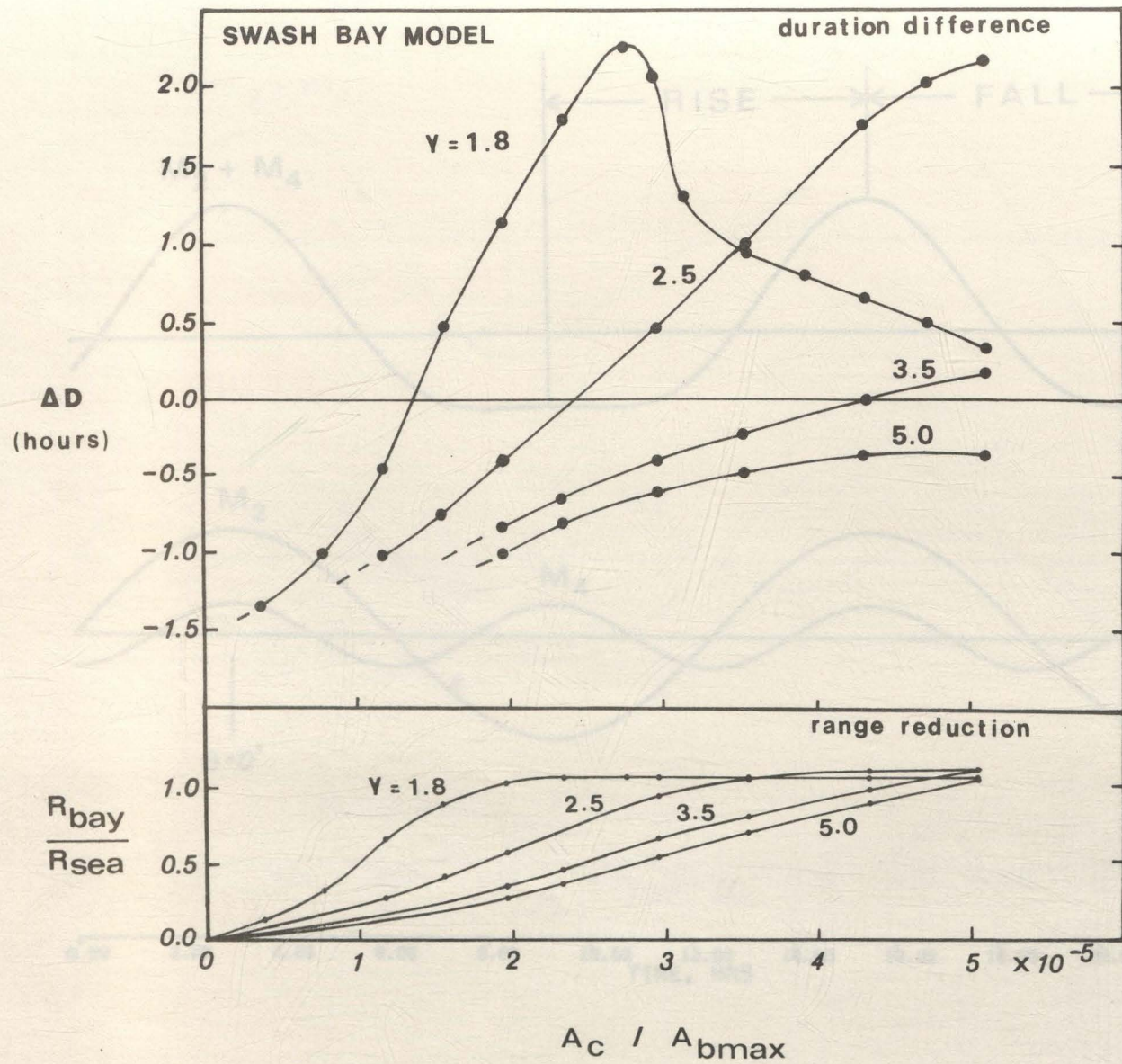
$$L'_i = \frac{L_{i,1} + L_{i,2}}{2}$$

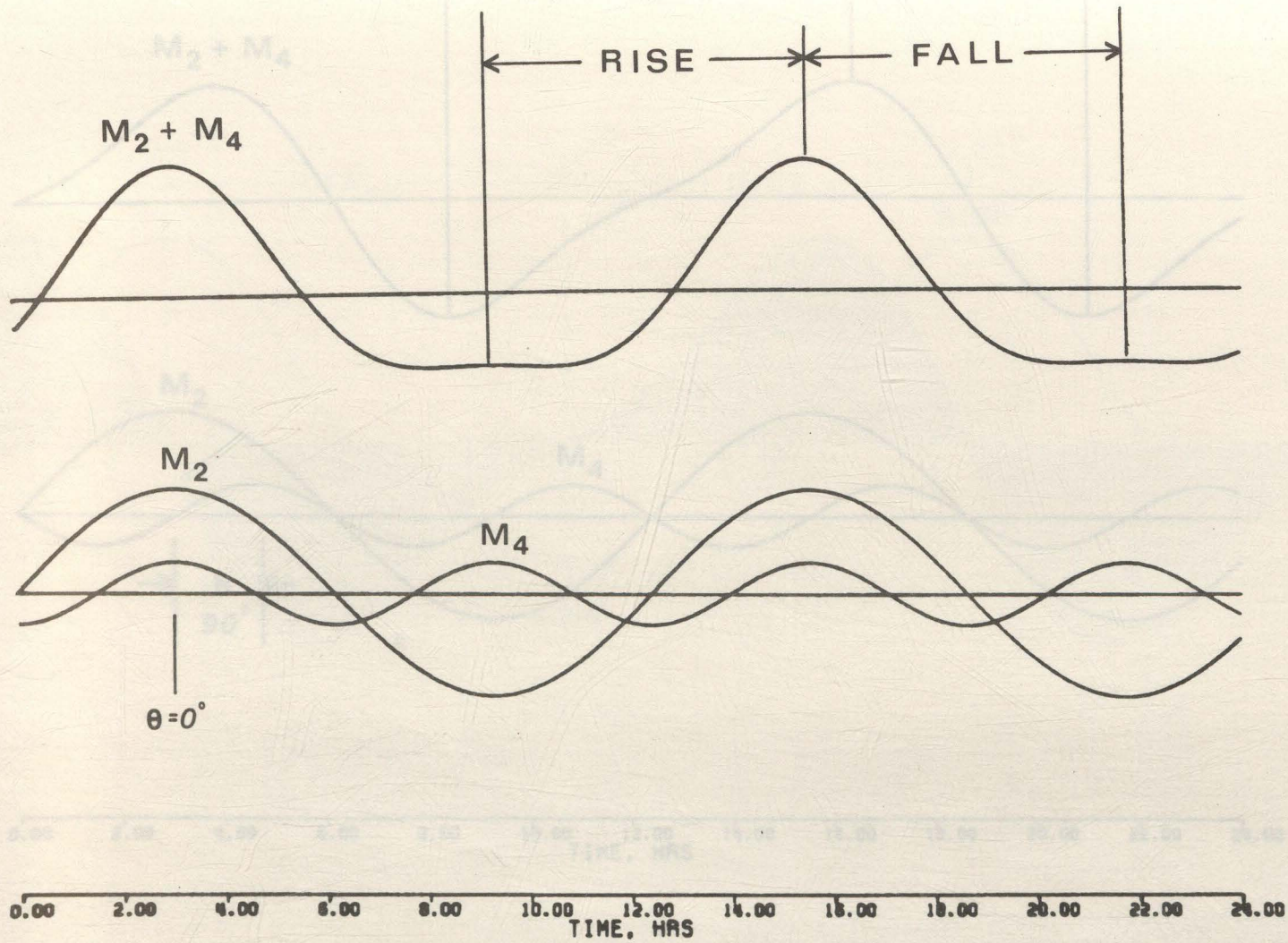
$$D_i = A'_i / B'_i$$

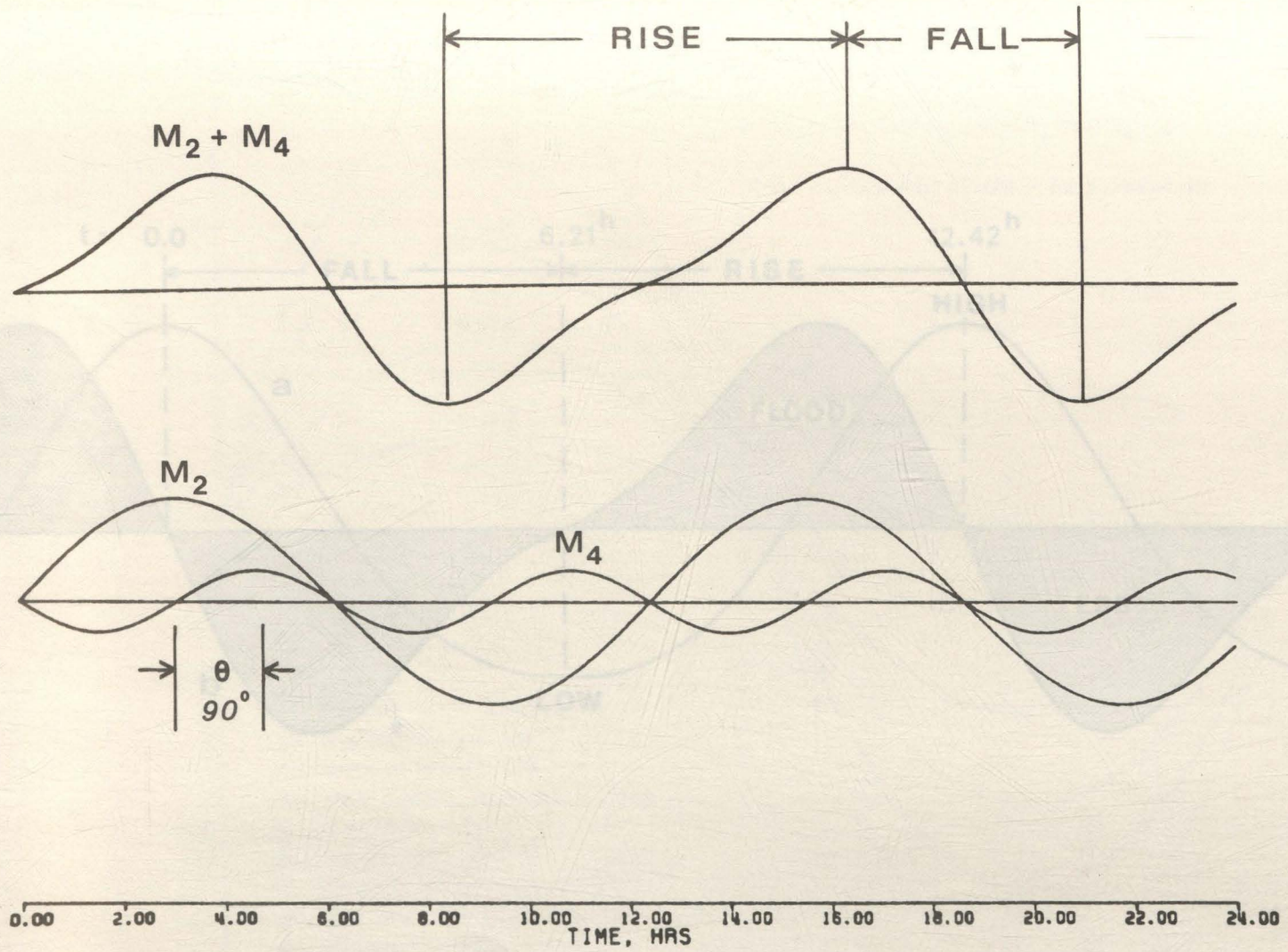


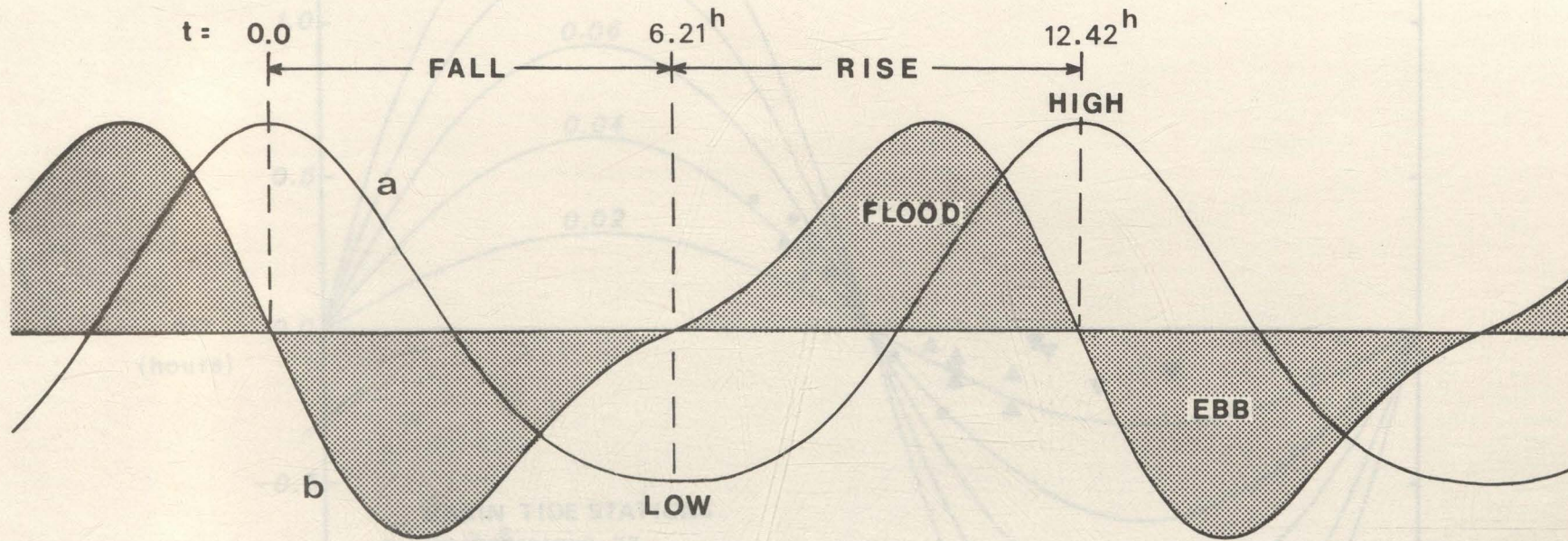












$M_4/M_2 = 0.14$

$h(t) = M_2 \cos \alpha_2 + M_4 \cos(\alpha_4 - \theta)$

$\Delta D = \text{rise duration} - \text{fall duration}$

OCEAN TIDE STATIONS

0 90 180 270 360

DEWEY

